Angewandte Chemie
Eine Zeitschrift der Gesellschaft Deutscher Chemiker

Supporting Information

Supramolecular Organization and Functional Implications of K^+ Channel Clusters in Membranes

*Koen M. Visscher, João Medeiros-Silva, Deni Mance, João P. G. L. M. Rodrigues, Mark Daniëls, Alexandre M. J. J. Bonvin, Marc Baldus, and Markus Weingarth**

anie_201705723_sm_miscellaneous_information.pdf
anie_201705723_sm_Supporting_Video1.avi
anie_201705723_sm_Video1.avi

Table of contents:

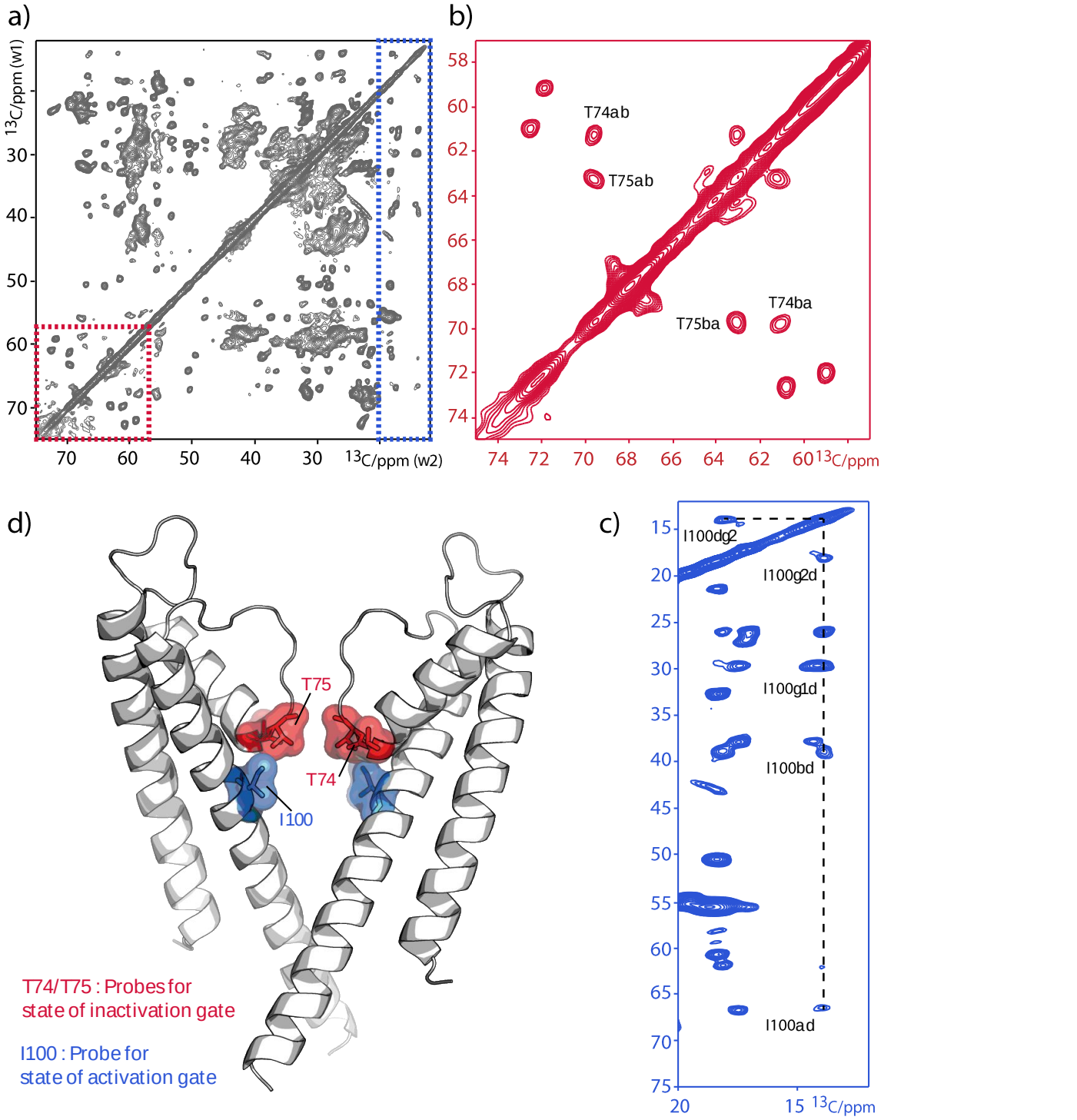

Figure S1. Cutouts of a) a 2D ^{13}C-^{13}C PARIS[1] spectrum, measured with full-length KcsA, showing signal patterns that are characteristic[2-5] for b) the *conductive* inactivation gate (also called selectivity filter) and c) the *closed* activation gate. d) Illustration of the molecular positions of the spectral probes (T74, T75, and I100) for the gating mode of KcsA.

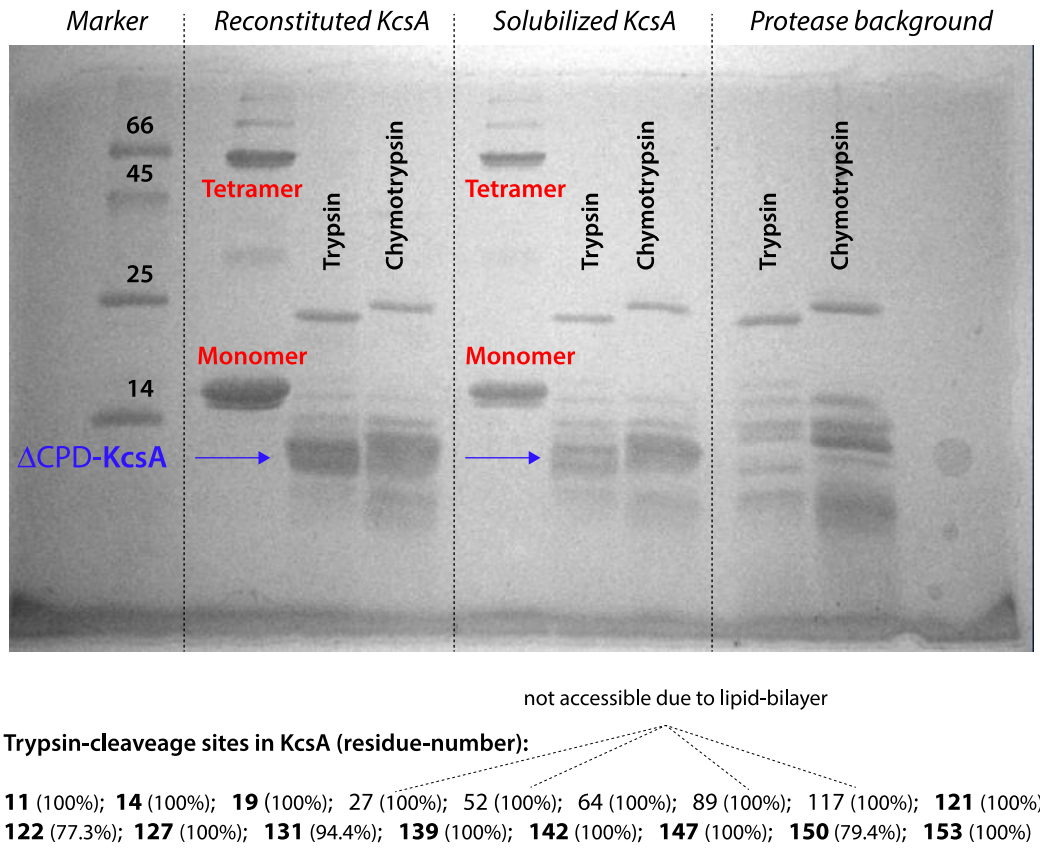

Figure S2. In accordance with previous reports,[6,7] an enzymatic cleavage assay reveals parallel topology of KcsA channels in our reconstituted liposome samples. The Figure shows SDS-PAGE on a 12.5% acrylamide gel: the marker in the first lane; left columns for KcsA reconstituted in lipid vesicles; middle columns for KcsA solubilized with decyl-β-D-maltoside [8]; right columns the protease background.

Treatment of reconstituted KcsA channels with proteases resulted in an almost homogenous truncated construct of about 10 - 12 kDa, consistent with a uniform cleavage of the C-terminal cytoplasmic domain (CPD), resulting in the dissociation of KcsA subunits. The parallel KcsA topology is illustrated by the complete lack of intact tetramers and monomers of KcsA, which would be present if channels adopted an antiparallel or random orientation that inhibited cleavage of the CPDs for a certain number of channels. The size of the ΔCPD-KcsA construct is highlighted by protease treatment of randomly orientated, DM-solubilized KcsA, which leads to a complete cleavage of the hydrophilic CPD. The position of trypsin-cleavage sites which are accessible for the enzymes are shown in bold. Analogously, cleavage sites of Chymotrypsin are restricted to the C- and N-termini.

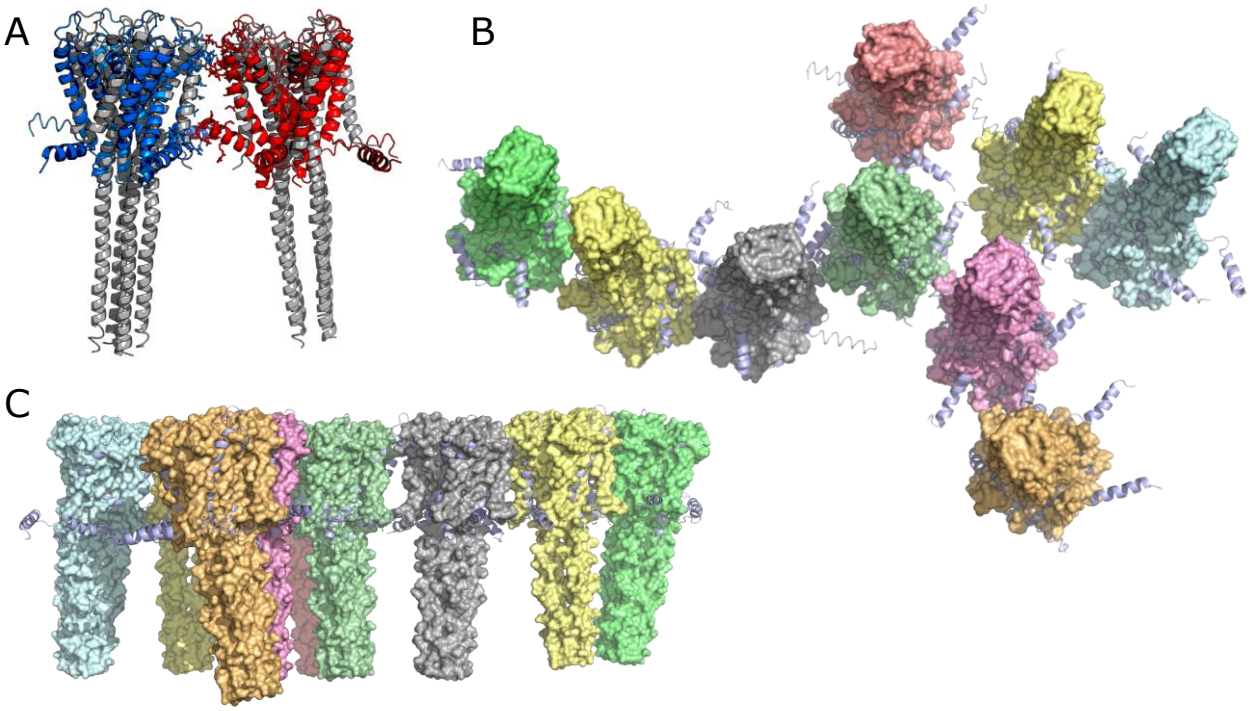

Figure S3. (A) Alignment of full-length KcsA crystal structures (pdb code 3EFF)[9] to a KcsA dimer that is representative for the contact map of Figure 3D. The KcsA dimer was taken from the end of the 37.5 μs CGMD simulation (Figure 3B) and back-transformed to atomistic coordinates using the Backward[10] tool. As can be seen from the alignment, the C-terminal cytoplasmic domains (CPDs; residues 125 – 160) of KcsA channels in clusters are far away from each other, which is also evident in (B) and (C), showing the same superposition for a larger ensemble of nine simulated KcsA channels from two different perspectives. This is in good agreement with previous studies, which reported that CPDs are neither necessary for nor involved in KcsA clusters.[11,12]

Supporting Video 1. The evolution of the 16 coarse-grained KcsA channels in presence of the M0 helix in *E. coli* lipids over 37.5 μs. Lipids, water and ions are left out for clarity. The time-resolution of the video is 100 ns. The coloring of the channels is arbitrary.

Experimental section

Sample preparation. The uniformly (U) $^{13}C^{14}N$ or $^{12}C^{15}N$ labeled KcsA samples were expressed in a medium containing U-^{13}C or U-^{12}C glucose and $^{14}NH_4Cl$ or $^{15}NH_4Cl$, respectively. Purification and reconstitution steps were done following earlier work (refs.[13,14]). Ion channels were reconstituted in *E. coli polar* lipids (Avanti) using a protein/lipid (P/L) molar ratio of 1/100 and 1/400 for conventional and DNP-enhanced ssNMR experiments, respectively. For the conventional ssNMR experiments, the reconstituted samples were washed twice for 1.5h in 50 mM K^+ / 50 mM Na^+/ 50 mM Na^+ / phosphate buffer (pH 7). For DNP-ssNMR experiments, the KcsA liposome sample was re-suspended in a 50 µl solution containing the biradical AMUPol.[15] The solution consisted of 1:2:2 (v/v/v) d_8-glycerol:D_2O:H_2O and 15mM AMUPol and the buffer conditions pH7: 50mM NaPi, 50mM NaCl, 50mM KCl or pH 4: 10mM Na_3 citrate and 120mM NaCl. Subsequently the sample was pelleted by centrifuging at 130,000g for 30 min. After removal of the supernatant, this procedure was repeated one more time. Afterwards the pellet was packed into a 3.2 mm sapphire rotor.

Solid-state NMR spectroscopy. *Conventional ssNMR.* NHHC[16,17] experiments were carried out in a magnetic field of 16.4 T (700 MHz ^1H frequency, Bruker BioSpin) and a magic angle spinning (MAS) frequency of 7.2 kHz, respectively. The second and third cross-polarization steps of NHHC experiments were kept short (100 - 300 µs). The effective sample temperature was set to 255 K, unless indicated otherwise. A 2D ^{13}C-^{13}C PARIS spectrum [1,18] was acquired at 700 MHz and 12 kHz MAS at 270 K. *DNP-enhanced ssNMR.* DNP-enhanced NHHC experiments were carried out at a proton/electron frequency of 400 MHz/263 GHz (Bruker BioSpin). All DNP experiments were performed at 100 K using a MAS rate of 8 kHz. For the DNP-enhanced 2D NHHC experiment, we used very short (100 µs) contact times for the second and third cross-polarization steps and a ^1H-^1H spin diffusion time of 600 µs. For the spectral comparison of DNP-enhanced 1D NHHC spectra of closed and open channels (Figure 2A,B), we scaled the spectra according to their intensities (see below). Importantly, we used the same sample preparation for the data acquired in Figure 2A,B. Samples were centrifuged out of the rotor and washed twice with acid (pH4) or neutral (pH7) buffers to obtain open or closed channels, respectively. Afterwards, samples were centrifuged back into a 3.2 mm sapphire rotor.

Comparison of the DNP spectra shown in Figure 2A,B of the main text: In Figures 2A,B of the main text, we compared signal intensities of 1D NHHC spectra of open and closed channels. Since the sample was washed with different buffers to *'shuttle'* the channels between closed and open states, the ratio of ^{13}C and ^{15}N labeled channels was the same for each experiment. However, it was necessary to scale intensities for the comparison due to i) different DNP-enhancements, and ii) loss of sample after the washing steps. To scale the spectra, we measured and compared intensities of DNP-enhanced 1D ^{15}N cross-polarization spectra for each buffer condition. These scaling factors were applied to each experimental series shown in Figures 2A,B.

Molecular Dynamics simulations. CGMD simulations were carried out using the GROMACS package version 4.5.4[19] and the MARTINI force field version 2.2[20] together with an integration step of 20 fs and the standard settings[20] for nonbonded interactions in a NPT ensemble. For nonbonded interactions, we used the potentials described in in the original MARTINI paper,[20] i.e., potentials for LJ and Coulomb interactions that are shifted (using the Gromacs shifting function) to zero between 0.9 – 1.2 nm and 0.0 - 1.2 nm, respectively. The system was semi-isotropically coupled to a pressure bath at 1 bar (τ_p = 3 ps) using the Berendsen Barostat[25] and coupled (τ_T = 0.3 ps) to a heat bath using the Berendsen Thermostat[25]. A solvated mixed DOPE : DOPG : Cardiolipin (7 : 2 : 1 molar ratio) bilayer, consisting of 205 DOPE, 59 DOPG lipids and 30 Cardiolipin, together with 4415 water beads and 95 sodium counter ions was equilibrated and one KcsA channel inserted. This system was expanded four times in both x and y dimensions, yielding a total system of dimensions 42.8 x 42.8 x 9.3 nm^3 (xyz) and a total number of beads of 158080. Cardiolipin parameters were taken from (ref. [21]). The CG KcsA structure was derived from a closed-conductive channel (pdb code 1K4C[22]) using the martinize.py script. An elastic network approach[23] with a force constant of 1000 kJ mol^{-1} nm^{-2} and a cutoff of 0.9 nm was used together with the MARTINI force field to ensure long-time stability of the protein fold. Independent elastic networks were used for each of the four KcsA subunits. No elastic bonds were applied between M0 helix and TM part of KcsA. The M0 helix was modelled using secondary structure restraints in MODELLER v9.12.[24]

References

(1) Weingarth, M.; Bodenhausen, G.; Tekely, P. *J Am Chem Soc* **2009**, *131*, 13937.

(2) Lange, A.; Giller, K.; Hornig, S.; Martin-Eauclaire, M. F.; Pongs, O.; Becker, S.; Baldus, M. *Nature* **2006**, *440*, 959.

(3) Ader, C.; Schneider, R.; Hornig, S.; Velisetty, P.; Wilson, E. M.; Lange, A.; Giller, K.; Ohmert, I.; Martin-Eauclaire, M. F.; Trauner, D.; Becker, S.; Pongs, O.; Baldus, M. *Nat Struct Mol Biol* **2008**, *15*, 605.

(4) Schneider, R.; Ader, C.; Lange, A.; Giller, K.; Hornig, S.; Pongs, O.; Becker, S.; Baldus, M. *J Am Chem Soc* **2008**, *130*, 7427.

(5) Wylie, B. J.; Bhate, M. P.; McDermott, A. E. *Proc Natl Acad Sci U S A* **2013**, *111*, 185.

(6) Cuello, L. G.; Romero, J. G.; Cortes, D. M.; Perozo, E. *Biochemistry* **1998**, *37*, 3229.

(7) Heginbotham, L.; LeMasurier, M.; Kolmakova-Partensky, L.; Miller, C. *J Gen Physiol* **1999**, *114*, 551.

(8) Gradmann, S.; Ader, C.; Heinrich, I.; Nand, D.; Dittmann, M.; Cukkemane, A.; van Dijk, M.; Bonvin, A. M.; Engelhard, M.; Baldus, M. *J Biomol NMR* **2012**, *54*, 377.

(9) Uysal, S.; Vasquez, V.; Tereshko, V.; Esaki, K.; Fellouse, F. A.; Sidhu, S. S.; Koide, S.; Perozo, E.; Kossiakoff, A. *Proc Natl Acad Sci U S A* **2009**, *106*, 6644.

(10) Wassenaar, T. A.; Pluhackova, K.; Bockmann, R. A.; Marrink, S. J.; Tieleman, D. P. *J Chem Theory Comput* **2014**, *10*, 676.

(11) Molina, M. L.; Barrera, F. N.; Fernandez, A. M.; Poveda, J. A.; Renart, M. L.; Encinar, J. A.; Riquelme, G.; Gonzalez-Ros, J. M. *J Biol Chem* **2006**, *281*, 18837.

(12) Sumino, A.; Yamamoto, D.; Iwamoto, M.; Dewa, T.; Oiki, S. *J Phys Chem Lett* **2014**, *5*, 578.

(13) Lange, A.; Giller, K.; Hornig, S.; Martin-Eauclaire, M. F.; Pongs, O.; Becker, S.; Baldus, M. *Nature* **2006**, *440*, 959.

(14) van der Cruijsen, E. A.; Nand, D.; Weingarth, M.; Prokofyev, A.; Hornig, S.; Cukkemane, A. A.; Bonvin, A. M.; Becker, S.; Hulse, R. E.; Perozo, E.; Pongs, O.; Baldus, M. *Proc Natl Acad Sci U S A* **2013**, *110*, 13008.

(15) Sauvee, C.; Rosay, M.; Casano, G.; Aussenac, F.; Weber, R. T.; Ouari, O.; Tordo, P. *Angew Chem Int Ed Engl* **2013**, *52*, 10858.

(16) Etzkorn, M.; Bockmann, A.; Lange, A.; Baldus, M. *Journal of the American Chemical Society* **2004**, *126*, 14746.

(17) Lange, A.; Luca, S.; Baldus, M. *Journal of the American Chemical Society* **2002**, *124*, 9704.

(18) Weingarth, M.; Demco, D. E.; Bodenhausen, G.; Tekely, P. *Chem Phys Lett* **2009**, *469*, 342.

(19) Hess, B.; Kutzner, C.; van der Spoel, D.; Lindahl, E. *J Chem Theory Comput* **2008**, *4*, 435.

(20) de Jong, D. H.; Singh, G.; Bennett, W. F. D.; Arnarez, C.; Wassenaar, T. A.; Schafer, L. V.; Periole, X.; Tieleman, D. P.; Marrink, S. J. *J Chem Theory Comput* **2013**, *9*, 687.

(21) Dahlberg, M. *J Phys Chem B* **2007**, *111*, 7194.

(22) Zhou, Y.; Morais-Cabral, J. H.; Kaufman, A.; MacKinnon, R. *Nature* **2001**, *414*, 43.

(23) Periole, X.; Cavalli, M.; Marrink, S. J.; Ceruso, M. A. *J Chem Theory Comput* **2009**, *5*, 2531.

(24) Sali, A.; Blundell, T. L. *J Mol Biol* **1993**, *234*, 779.

(25) Berendsen, H.J.C., Postma, J.P.M., van Gunsteren, W.F., DiNola, A., Haak, J.R. *J Chem Phys* **1984**, 81, 3684